

# BULLETIN

## OF THE KOREAN CHEMICAL SOCIETY

VOLUME 9, NUMBER 4  
AUGUST 20, 1988

BKCS 9(4) 191-270 (1988)  
ISSN 0523-2964

### Some Thiosemicarbazide Derivatives as Corrosion Inhibitors for Aluminium in Sodium Hydroxide Solution

M.N. Moussa, A.S. Fouda\*, F.I. Taha, and A. Elnenaa

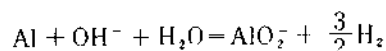
*Chemistry Department, Faculty of Science, Mansoura University, Mansoura, Egypt*

*Received February 4, 1987*

The effect of some thiosemicarbazide derivatives on corrosion of aluminium in 2M sodium hydroxide has been studied using thermometric, weight loss and hydrogen evolution techniques. The rate of the corrosion depends on the nature of the inhibitor and its concentration, heated of hydrogenation, mode of interaction with the metal surface and formation of metallic complexes. The compounds are weakly adsorbed on the surface of aluminium and form a monolayer of the adsorbate. Values of the Arrhenius activation energies indicate agreement with those obtained for an activation controlled process.

#### Introduction

Aluminium and its alloys find extensive applications in mechanical and chemical environments as components in pumps, valves, textiles and marine industries. It is known that the dissolution of aluminium in alkaline solution is represented by:



In earlier communications<sup>2,3</sup> it was found that thiosemicarbazide derivatives inhibit the corrosion of aluminium in hydrochloric acid and sodium hydroxide solutions. Also, Fouda<sup>4</sup>, Issa<sup>5</sup> and Mostafa<sup>6</sup> used thiosemicarbazide and its derivatives as corrosion inhibitors of some metals. In the present study various measurements are used to compare the inhibition effect of thiosemicarbazide derivatives on the dissolution of aluminium in sodium hydroxide. Kinetic studies on the dissolution reaction were also carried out.

#### Experimental

**Materials.** Thiosemicarbazide derivatives used as inhibitors were prepared<sup>7</sup> by adding slowly the appropriate volume of phenyl isothiocyanate to the corresponding acid hydrazide in absolute ethanol. The purity of all the additives was checked by melting point determinations. 2M sodium hydroxide solution was prepared by dilution from car-

bonate-free stock solution. The additive solutions were prepared by dissolving the required amounts of each in cold or hot 2M sodium hydroxide. Degreasing mixture was prepared as previously described<sup>8</sup>.

The chemical composition of the aluminium sheet used was as follows: Si: 0.15, Fe: 0.19, Mn: 0.005, Mg: 0.1, Cu: 0.02, Al: 99.535% and the dimensions of the test pieces in thermometric method were 1 × 10 × 0.2cm, where as in weight loss and hydrogen evolution the dimensions were 2 × 2 × 0.2 cm. These were cleaned and degreased as previously described<sup>9</sup>.

**Apparatus and Working Procedures.** The reaction vessel used was basically the same as that described by Mylius<sup>10</sup>. According to this method, a test piece of the metal under study, measuring 1 × 10 × 0.2cm, is immersed in 15ml of 2M NaOH in presence and in absence of the additives and the temperature of the system is followed as a function of time. The temperature rises, first slowly and then rapidly, to attain a maximum value and then decreases again. The reaction number RN is defined as:

$$\text{RN} = \frac{T_m - T_i}{t} \text{ } ^\circ\text{C}/\text{min}$$

where  $T_m$  and  $T_i$  are the maximum and initial temperatures respectively and  $t$  is the time in minutes from the start of the experiment till the attainment of maximum temperature. The initial temperature was always  $30 \pm 0.2^\circ\text{C}$ .

The procedure followed in weight loss measurements was similar to that reported previously<sup>9</sup>. The percentage inhibition of the additives was computed as:

\*To whom correspondence should be addressed.

Present address: Chemistry Department, Qatar University, Qatar, Doha P.O. Box 2713.

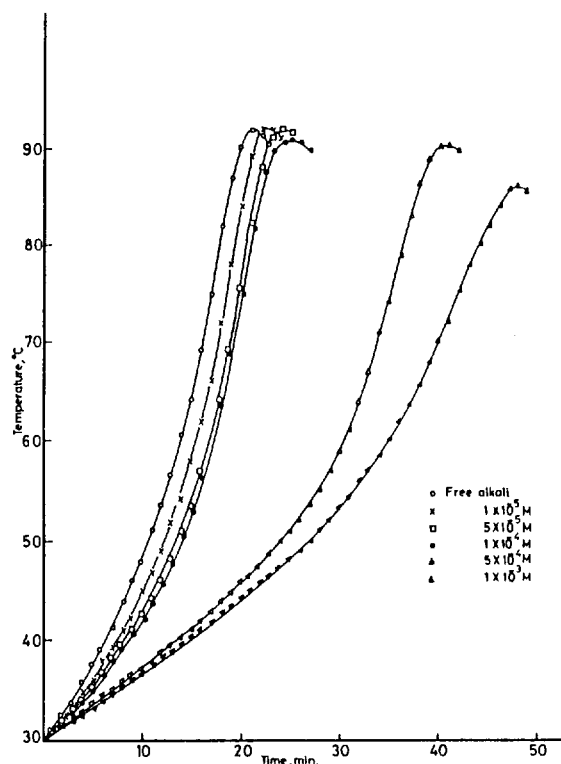


Figure 1. Temperature-time curves obtained in absence and in presence of varying concentrations of compound III.

$$100 \left( \frac{W_{\text{free}} - W_{\text{add}}}{W_{\text{free}}} \right)$$

where  $W$  is the loss in weight of the test piece.

In hydrogen evolution method, the vessel was the same as that used before<sup>11</sup>. A weighed aluminium sample was dropped into 100ml of 2M NaOH at 30°C and the volume of hydrogen evolved was recorded to  $\pm 0.05$  ml as a function of time. The efficiency of a given inhibitor was evaluated as the percentage reduction in reaction rate, viz.

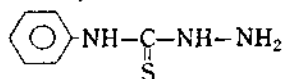
$$\% \text{ reduction in RR} = \left( \frac{R_{\text{free}} - R_{\text{add}}}{R_{\text{free}}} \right) 100$$

where  $R_{\text{free}}$  and  $R_{\text{add}}$  are the rates of aluminium dissolution in free alkali and in presence of the given inhibitor respectively, both measured at the same time.

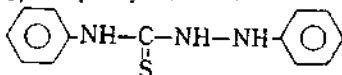
## Results and Discussion

The thiosemicarbazide derivatives used as corrosion inhibitors in this investigation are as follows:

(I) 4-Phenyl-3-thiosemicarbazide



(II) 1,4-Diphenyl-3-thiosemicarbazide



(III) 4-Phenyl-(2,4-dinitrophenyl)-1,3-thiosemicarbazide

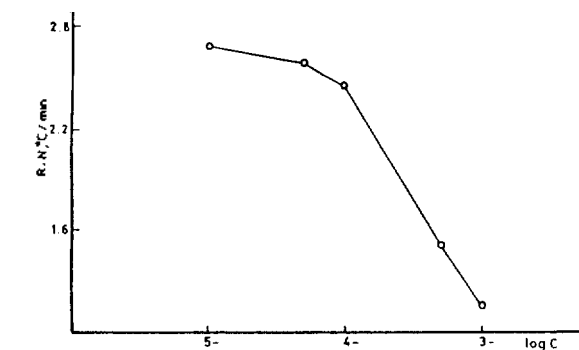
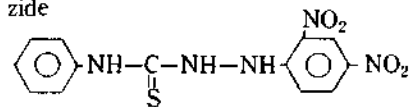
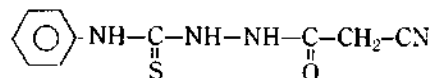
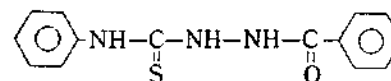


Figure 2. Variation of reaction number RN with the logarithm of concentration of compound III in alkaline solution.

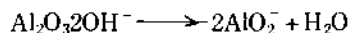
(IV) 4-Phenyl-1-cyanoacetyl-3-thiosemicarbazide



(V) 4-Phenyl-1-benzoyl-3-thiosemicarbazide



The curves of Figure 1 represent the variation of temperature of the system with time in presence and in absence of different concentrations of inhibitor III as an example. It is evident that the dissolution of aluminium in 2M NaOH starts from the moment the metal is introduced into the corroding solution. An incubation period<sup>12</sup> is first recognized along which the temperature rises gradually with time. Aluminium, as an active element, always carries an air formed oxide with spinel structure<sup>13</sup> which specifically and very strongly adsorbs  $H^+$  and  $OH^-$  ions<sup>13</sup>. So, when aluminium is introduced into an alkaline solution the  $OH^-$  ions are primarily adsorbed on its surface. Due to the acidic property of the oxide film it is chemically attacked in a reaction of the type:



This reaction takes place along the incubation period. The heat evolved from the above reaction accelerates further dissolution of the oxide and activates the dissolution of the metal exposed to the aggressive medium. The curves of Figure 1 also show that as the concentration of the additive increases the time required to reach the maximum temperature ( $T_m$ ) increases and the rate of temperature rise decreases, i.e., the inhibition efficiency increases with the increase in concentration of additives. The present thermometric curves allow distinction between weak and strong adsorption<sup>14</sup>. Weak adsorption is noted for all inhibitors used. Figure 1 represent this adsorption in the presence of compound III, in which the maximum temperature slightly decreases whilst the time necessary to reach  $T_m$  increases.

Figure 2 exhibits the relation between the reaction number RN and the logarithm of molar concentration ( $C$ ) of inhibitor (III). Similar curves are obtained for the different additives used. The curves consist of an initial decreasing portion along which the RN decreases with increasing the inhibitor concentration then the rate of decrease becomes smaller. As the concentration of the additive increases further the values of RN decreases linearly with concentration. It is evident that all the tested compounds form a monolayer

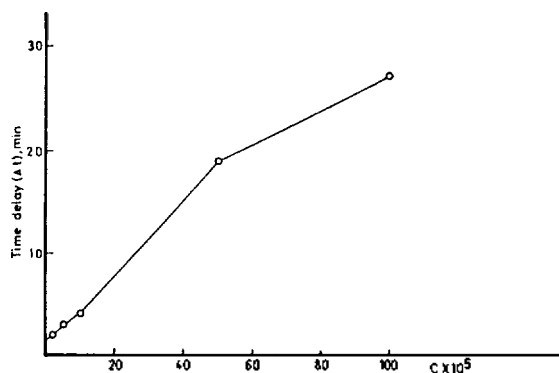


Figure 3. Time delay ( $\Delta t$ ) vs. concentration of compound III in alkaline solution.

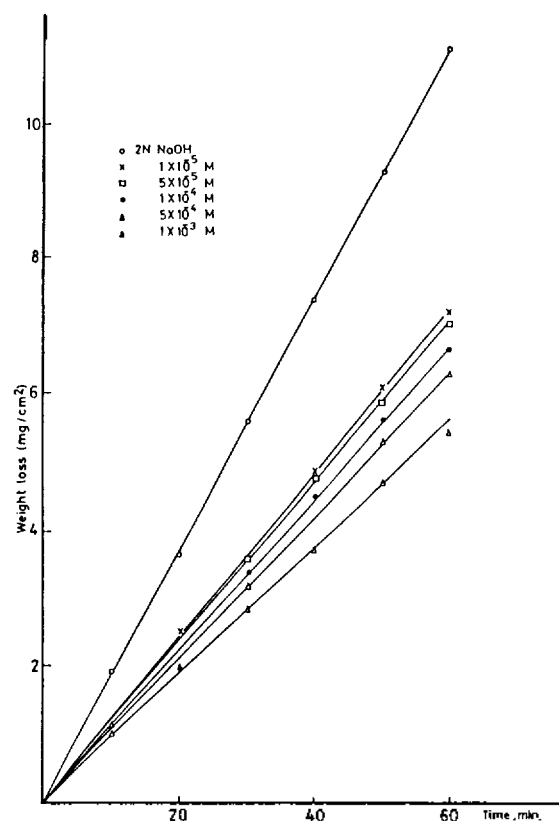


Figure 4. Weight loss-time curves for compound III.

on the surface of aluminium. Also curves of the time delay ( $\Delta t$ ) vs. concentration (Figure 3) [time delay ( $\Delta t$ ) is the difference between  $T_m$  in presence of the additive and  $T_m$  in absence of the additive]. These curves consist of an initial linear portion which passes to a region of constancy indicating the completion of a monolayer of the adsorbate. The order of decreased inhibition efficiency of the additives as determined by the % reduction in RN At  $1 \times 10^{-3} M$  in alkaline medium is: III > V > IV > II > I > thiosemicarbazide.

Weight loss in  $\text{mg cm}^{-2}$  of the surface area were determined in an open system at various time intervals in absence and in presence of the inhibitors. Representative curves for the system involving inhibitor III are shown in Figure 4. The curves are straight lines starting from the origin and weight losses gradually increase by increasing time. Curves for ad-

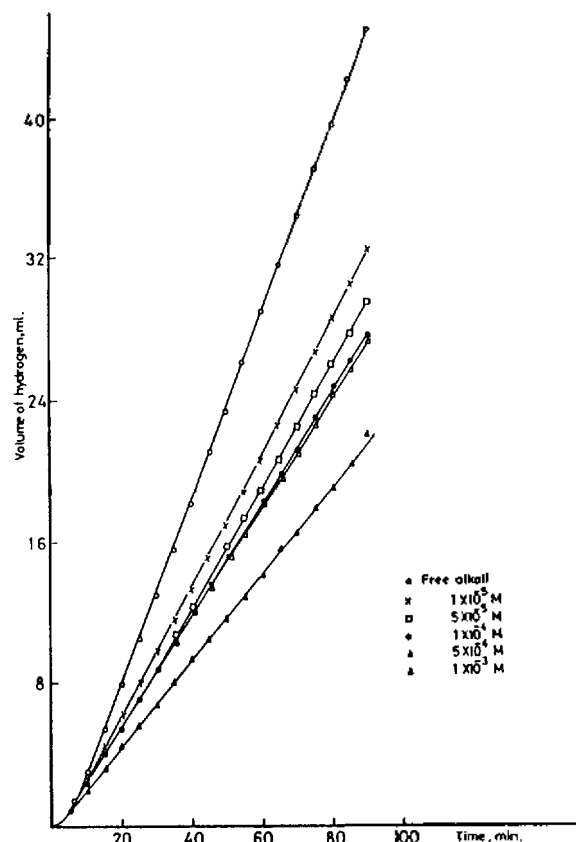


Figure 5. Volume of hydrogen-time curves for compound III.

divites containing systems fall below that of the free alkali. These curves indicate that weight loss of Al depends on both the type and concentration of the additives, and the % inhibition increases with concentration due to the increase in the surface area covered with the additive. The order of decreased inhibition efficiency of the additive compounds at  $1 \times 10^{-3} M$  given by weight loss measurements in alkali solution is: III > V > IV > II > I thiosemicarbazide.

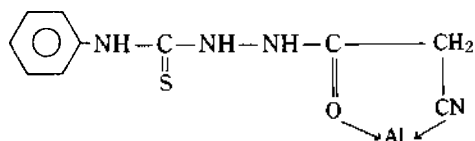
The volume of hydrogen evolved-time curves at constant temperature ( $30^\circ\text{C}$ ) in presence and in absence of different concentrations of inhibitor III, as an example are represented in Figure 5. There is an initial slow increase in the volume of hydrogen evolved with time and finally the curves become linear with time. The first of the curve may be due to the oxide film originally present on the metal surface. The results obtained indicate that on increasing the inhibitor concentration the % reduction in RR increases and depends also upon the type of the inhibitor. The results reveal that in alkali solution at  $1 \times 10^{-3} M$  concentration of additives the order of decreased corrosion inhibition efficiency is: III > V > IV > II > I > thiosemicarbazide.

The inhibition efficiency of additive compounds depend on many factors which include the molecular size, heat of hydrogenation, mode of interaction with the metal surface, formation of metallic complexes and the charge density on the adsorption sites. As reported before<sup>15,16</sup>, the inhibition efficiency in sodium hydroxide solution is very low. Adsorption is expected to take place primarily through a functional groups, essentially C=S and C=O and would depend on its charge density. Compound I is a more effective inhibitor than thiosemicarbazide due to the presence of a phenyl group

**Table 1. Comparison between Efficiency of Inhibitors as Determined by Thermometric, Weight Loss and Hydrogen Evolution Techniques in Alkaline Solution at  $1 \times 10^{-3}$  Concentration at  $30 \pm 0.2^\circ\text{C}$**

Compound	% Reduction in RN	% Inhibition	% Reduction in RR
Free alkali	—	—	—
III	60.6	51.1	50.9
V	59.4	37.7	46.0
IV	56.8	37.4	43.0
II	42.0	30.1	43.8
I	40.9	29.6	42.6
Thiosemicarbazide	37.1	26.0	41.2

which increases the molecular size of the compound leading to a larger surface coverage of Al. Compound II has two phenyl groups as is consequently more effective than I. Both the thiosemicarbazide derivatives III and V have also two phenyl groups but they come on top of the series in inhibition efficiency due to larger molecular size imported from the presence of the 1-(2,4-dinitrophenyl) and 1-benzoyl substituents respectively. However, compound III appears to be more effective than V evidently because of larger molecular size. Delayed hydrogenation in alkaline medium of the nitro groups III would not aid much the desorption of the compound. The carbonyl group in V is also susceptible to hydrogenation. The 4-phenyl-1-cyanoacetyl derivative IV comes after III and V in the sequence of inhibition efficiency and this may be due to a favourable interaction with the surface leading to the formation of an aluminium complex of the type:



which is obviously less soluble in alkaline than in acid medium<sup>2</sup>.

Table 1 collects and compares the results obtained by the three different techniques employed for evaluating the extent and order of corrosion inhibition efficiencies of thiosemicarbazide and its derivatives for aluminium dissolution in NaOH solution. The agreement observed among them confirms the validity of the present measurements. These results also support the explanation given for the effect of chemical composition on the inhibitive action of the investigated compounds.

The dissolution of aluminium itself is linearly related to the reaction time (at  $30^\circ\text{C}$  and after 10 min from beginning). This is observed from the curves in Figure 5. This behaviour is an indication of zero order reaction with general equation:

$$x = kt$$

where  $x$ , the fraction of aluminium dissolved at time  $t$ , is directly proportional to the volume of hydrogen evolved at time  $t$  and  $k$  is the rate constant of the reaction. The values of  $k$  can be calculated from the slope of the  $x-t$  curves at the given temperature. In this manner the rate constants of

**Table 2. The Specific Rate Constants ( $k$ ) of Aluminium Dissolution in 2*N* NaOH in Presence and in Absence of Inhibitors at  $1 \times 10^{-3}M$  Concentration**

Compound	Temperature, $^\circ\text{C}$				$E$ , kcal/( $\text{mg}/\text{cm}^2$ ) $\pm 0.03$
	30	40	50	60	
Free alkali	0.317	0.828	1.407	2.591	14.09
III	0.231	0.432	1.346	2.357	15.18
V	0.073	0.579	1.163	2.079	19.74
IV	0.401	0.666	1.453	2.614	13.13
II	0.211	0.689	1.345	2.588	14.18
I	0.297	0.775	1.326	2.647	14.27
Thiosemi-carbazide	0.297	0.775	1.326	2.647	14.27

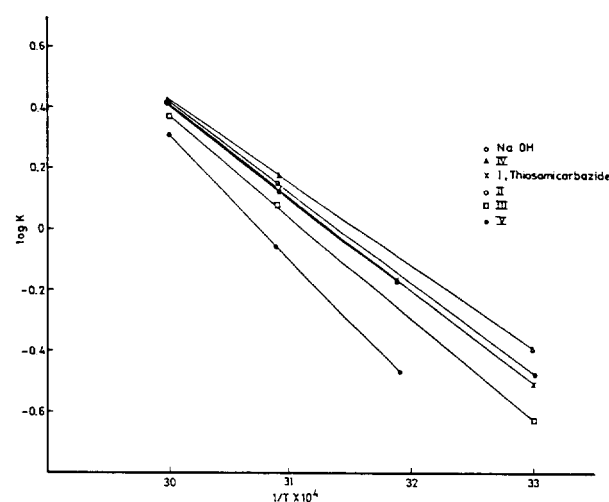


**Figure 6. Log  $k$ - $1/T$  curves for aluminium dissolution presence and in absence of different inhibitors.**

aluminium dissolution in NaOH and in presence of the inhibitors (Table 2) were determined. It is evident that the rate constant increases with rise in temperature and is accompanied by a decrease in the inhibition efficiency of the additives. Therefore, the values of the rate constant can also be used for comparing the inhibition efficiencies of the inhibitors. The logarithm of rate constant of the reaction is a linear function of  $1/T$  (Figure 6). The Arrhenius activation energy values,  $E$ , obtained from the slopes of  $\log k$  vs  $1/T$  are presented in Table 2. These values increase with increasing inhibition efficiency of the additives and suggest that the process is activation controlled.

## References

- W. M. Latimer, "Oxidation Potentials," Printice Hall, New York, 168, (1953).
- A. S. Fouda, M. N. Moussa, F. I. Taha, and A. I. Elnanaa, *Corros. Sci.*, **26**, 719 (1986).
- A. S. Fouda, and A. A. Elasmay, *Monatsh Chem.*, **118**, 709 (1987).
- A. S. Fouda, H. Abu-Elnader, and M. N. Moussa, *Acta Chim. Ung.* in press.
- I. M. Issa, A. A. El-Samahy, and Y. M. Temark, *J.*

- Chem. U.A.R.*, **13**, 121 (1970).  
 6. A. B. Mostafa, Kh. M. Kamel, and I. A. Abdel Hamid, *Indian J. Chem.*, **15**, 1010 (1977).  
 7. A. A. Elasmay, Ph. D. Thesis, Mansoura University, Egypt (1981).  
 8. I. M. Issa, M. N. Moussa, and A. A. Elgandour, *Corros. Sci.*, **13**, 791 (1973).  
 9. K. Aziz, and A. M. Shams El-Din, *Corros. Sci.*, **5**, 489 (1965).  
 10. F. Z. Mylius, *Metalkade*, **14**, 233 (1922).  
 11. S. M. Hassan, Y. A. Elawady, and A. I. Ahmed, *Corros. Sci.*, **19**, 961 (1979).  
 12. J. M. Abdel Kader, and A. M. Shams Eldin, *Corros. Sci.*, **10**, 551 (1970).  
 13. M. Z. Pryor, *Electrochem.*, **62**, 782 (1958).  
 14. R. M. Saleh, and A. M. Shams El-Din, *Corros. Sci.*, **10**, 551 (1970).  
 15. A. S. Fouda, *Indian J. Techn.*, **20**, 412 (1982).  
 16. V. K. Subramanian, *Proc. 14th Semin Electrochem.*, **5**, 368 (1973).

## Convenient Synthesis of Chiral *trans*-2-Phenylcyclopropanecarboxylic Acid

Nam Sook Cho\*, Dae Hyun Shin, Chong Chul Lee, and Do Young Ra

Department of Chemistry, College of Natural Sciences Chungnam National University, Chungnam 302-764

Received February 24, 1987

(-)-(1R, 2R) and (+)-(1S, 2S)-menthyl-*trans*-2-phenylcyclopropanecarboxylate have been synthesized with the aid of chiral Cu(II) complex catalyst by the addition reaction of *l*-menthyl diazoacetate to styrene. The yield was 75%, with the purity of *trans* isomer over 95% and the optical purity of 95%.

### Introduction

For the syntheses of chiral cyclopropane derivatives have been utilized the reactions<sup>1,2</sup> of olefine with stoichiometric amounts of chiral sulfonium ylides, the Simmons-Smith reaction<sup>3-5</sup> (CH<sub>2</sub>X<sub>2</sub>/Zn) employing chiral substrates, or catalytic olefin cyclopropanation<sup>6-11</sup> with diazoalkanes under the influence of chiral metal complexes. The most desirable enantioselectivity has been achieved through asymmetric carbenoid reactions of diazo compounds catalyzed by bis( $\alpha$ -camphorquinonedioximate)cobalt (II) complex. Despite the high enantioselectivity, the cobalt catalyst system produced two geometrical isomers, *cis* and *trans*-2-phenylcyclopropanecarboxylate, in roughly comparable amounts. Chiral copper catalyst<sup>6</sup> was reported to show less enantioselectivity comparing with the cobalt catalyst, but it mainly produced *trans* isomer.

Thus, we decided to synthesize *trans*-2-phenylcyclopropanecarboxylic acid utilizing the copper catalyst. The synthesis of an optically active copper catalyst was patterned after the work of Aratani, Yoneyshi and Nagase on asymmetric synthesis of chrysanthemic acid. 2-Bromo-4-*tert*-butylphenyl *n*-octyl ether (**1**) was given by monobromination<sup>12</sup> of 4-*tert*-butylphenol followed by alkylation<sup>13</sup> with *n*-octyl bromide using potassium carbonate in acetone. The corresponding Grignard reagent was allowed to react<sup>14</sup> with (*R*)-alanine ethyl ester in tetrahydrofuran to give (2*R*)-1,1-diaryl-2-amino-1-propanol (**2**). This primary amine was condensed with salicylaldehyde (benzene, *p*-toluenesulfonic acid) to afford a salicylalimine (**3**) as a bright yellow oil. When this imine was treated with cupric acetate and aqueous sodium hydroxide in ethanol, there was obtained copper complex (**4**) as a viscous, dark green oil.

In the presence of this chiral copper catalyst, the addition reaction of *l*-menthyl diazoacetate to styrene produced a mixture of *cis* and *trans* ester (**5**). To measure the ratio of *trans* to *cis* isomer and the optical purity, NMR spectroscopy was employed after conversion to the methyl esters. The sequence of steps<sup>15</sup> used to convert menthyl esters to the corresponding methyl esters is outlined in Scheme 1. The ratio

